Supplement of

Optical properties and forcing efficiency of the organic aerosols and black carbon emitted by residential wood burning in rural Europe

Cuesta-Mosquera et al.

Correspondence to: Andrea Cuesta-Mosquera (cuesta@tropos.de, andrea.cuesta2305@gmail.com)

1. Principles of instrument operation

We provide a general description of the Aethalometer AE33 compensation algorithm, and operation principles of the Total Carbon Analyzer, MPSS, and Hi-Vol sampler used in the field campaign. For more specifications, the reader is referred to complementary studies and documentation from the instrument manufacturers (Drinovec et al., 2015; Magee Scientific, 2018; Wiedensohler, 1988).

1.1 Aethalometer AE33 algorithm

The calculations in the Aethalometer AE33 transform the change of the attenuation ($\Delta ATN_1(\lambda)$) into absorption coefficient ($b_{abs}(\lambda)$) using a correction factor for the multiple scattering of light (*C*, filter material dependent, Eq. S1) and additional variables: the spot area (*s*), the airflow through spot 1 (F_1), and a leakage factor (ζ). According to the manufacturer, the value of *C* depends on the filter material (Magee Scientific, 2018). However, various studies point out that the aerosol type also affects the scattering of light in filter-based absorption photometers. In a recent study, Drinovec et al. (2022) compared the AE33 attenuation to a newly developed Photothermal Aerosol Absorption Monitor (PTAAM), which measures at two wavelengths (532 and 1064 nm). The PTAAM was designed to eliminate light scattering artifacts during aerosol light absorption measurements. This characteristic favors the evaluation of artifacts in filter-based absorption photometers like the AE33. During field measurements, the PTAAM-AE33 comparison resulted in *C* factors of 3.28 (532 nm) and 2.57 (1064 nm); in laboratory analyses, *C* ranged between ~2.5 to ~5.5 depending on the volume size of soot particles (100 – 500 nm). In a field measurement campaign in Melpitz, Germany, collocated measurements of light absorption coefficients by AE33 and Multi-Angle Absorption Photometer (MAAP) showed that the light absorption estimated from the AE33 was between 10 and 100% above the MAAP absorption at 637 nm (interpolated for AE33). The overestimation has resulted in AE33-MAAP scaling factors ranging from 1.1 to 4.5 in Melpitz during periods of high residential wood-burning.

The dual-spot system of the AE33 is used to calculate a correction factor *k* to compensate for the filter-loading effect produced by the shadowing of particles accumulated on the filter. The absorption is loading-compensated ($b_{abs}(\lambda)^{comp.}$, Eq. S2), and used together with predetermined values of BC mass absorption cross sections ($MAC(\lambda)$) to estimate the mass concentrations of equivalent black carbon at multiple wavelengths ($eBC(\lambda)$, Eq. S3) (Drinovec et al., 2015).

$$b_{abs}(\lambda)^{non\ comp.} = \frac{s*(\Delta \mathrm{ATN}_1(\lambda)/100)}{F_1*(1-\zeta)*C*\Delta t}, \quad \text{(S1)}$$

$$b_{abs}(\lambda)^{comp.} = \frac{b_{abs}(\lambda)^{non\ comp.}}{(1-k(\lambda)*\mathrm{ATN}_1(\lambda))}, \quad \text{(S2)}$$

$$eBC(\lambda) = \frac{b_{abs}(\lambda)^{comp.}}{MAC(\lambda)}, \quad \text{(S3)}$$

1.2 Total Carbon Analyzer (TCA)

The Total Carbon Analyzer TCA08 estimates total carbon (TC) concentrations in aerosol particles using an online thermal method. The instrument integrates two analytical chambers which sequentially alternate between sample collection and sample analysis, i.e., while one chamber collects a new aerosol sample (sampling time ranging from 20 min to 24 h), the second chamber performs the thermal analysis of the sample previously collected (17 min for analysis). The aerosols are deposited on a quartz-fiber filter forming one sample-laden spot. Once the sample-collection period finishes, the filter is heated almost instantaneously up to 940 °C to combust all the carbonaceous compounds (organic carbon and elemental carbon). An infrared sensor measures the concentration of CO_2 present in the carrier gas (filtered ambient air) before ($CO_2^{ambient}$) and after (CO_2^{signal}) the combustion step. Subsequently, both concentrations are integrated over the heating time, together with the CO_2 from the blank filter (CO_2^{blank}) to estimate the total carbon concentration of the sample (Rigler et al., 2020).

1.3 Mobility Particle Size Spectrometer (MPSS)

The MPSS determines the particle number size distribution of atmospheric aerosol particles. The instrument contains three consecutive main components: a bipolar diffusion charger (neutralizer), a Differential Mobility Analyzer (DMA), and a Condensation Particle Counter (CPC). At first, the particles are led to a bipolar charge equilibrium through a radioactive source in the bipolar charger. The aerosols charged pass to the DMA, consisting of a cylindrical capacitor where the particles are separated according to their electrical mobility (Z_p). The electrical mobility depends on the particle charge, diameter, the corresponding Cunningham slip correction factor, and the gas viscosity. Since the shape and dimensions of the DMA are well known, it is possible to estimate and administer specific voltages to the electrodes to transport the particles with definite electrical mobilities from the entrance of the DMA to the annular slit in the center of the capacitor. The distribution of Z_p is determined by scanning the voltage over the entire range of electrical particle mobility of interest. Lastly, the CPC counts the number concentration of particles with specific Z_p. Small particles (diameter < ~100 nm) need a size enlargement to be optically detected in the CPC. In the butanol-type CPC, this is achieved by heating and saturation of the aerosol particles with butanol vapor; next, in a cooling section, the butanol condenses onto the particles and forms bigger droplets (~10 μm). The droplets are brought to a focusing nozzle, and an optical laser counts them individually (Wiedensohler et al., 2012, 2018). In the water-type CPC, the aerosols are preconditioned in a humid section of the tube, saturating the sample. Next, a heated section of the tube increases the water vapor pressure, supersaturating the sample, and condensation on the aerosol particles starts. Finally, a cooling section allows complete condensation and growth (TSI Inc, 2023).

1.4 Digitel sampler DHA-80

In the high-volume sampler Digitel DHA-80, the aerosol particles are continuously collected through a PM_{10} inlet and deposited over a circular filter collocated in the instrument flow chamber. The upper section of the flow chamber functions as a diffuser with a regular cross-section to guarantee uniform loading of the filters. During each sampling, the instrument measures the air flow transported through the filter (ranging from 100 to 1000 L min^{-1}) and records the total sampling time. The pressure drop across the filter is controlled, as well as the internal air pressure and temperature. The DHA-80 operates according to the standard EN12341 "ambient air – gravimetric method for determining the PM_{10} or $PM_{2.5}$ mass concentration of suspended particulate matter" (Digitel Enviro Sense, 2021).

2. OA/OC ratio

The OA/OC ratios in Retje, Loški Potok ranged between 0.8 and 4.4; Fig. S1 shows the histogram and the median value.

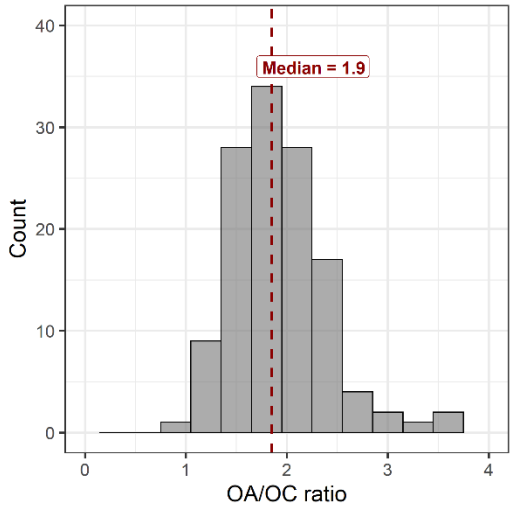

Figure S1. Frequency distribution of the OA/OC ratio.

3. Comparison of the calculated OA mass with OA mass from the Total Carbon Analyzer

Following the procedure from Rigler et al. (2020), the hourly organic carbon mass was calculated from the total carbon mass measured by the Total Carbon Analyzer (Eq. S4).

$$[OA]_{TCA} = ([TC]_{TCA} - [eBC]_{AE33}) * (OA/OC), \quad \text{(S4)}$$

The estimated hourly OA mass concentration (OA_{MPSS}) was compared against the OA mass from the Total Carbon Analyzer OA_{TCA} (Fig. S2).

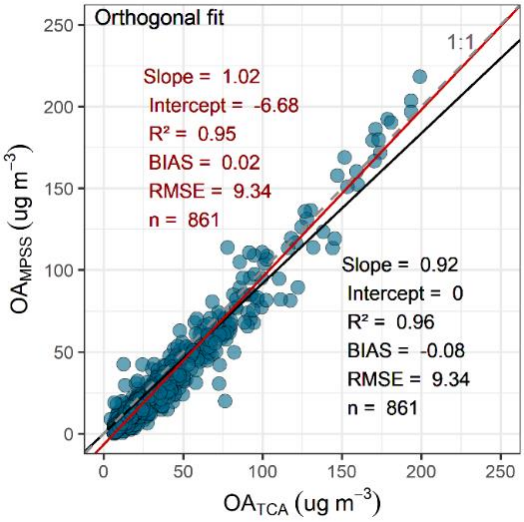

Figure S2: Scatter plot and orthogonal regressions with intercept (solid red line) and forced-to-zero intercept (solid black line) for the OA mass calculated from the MPSS (OA_{MPSS}) and the OA mass calculated from the TCA (OA_{TCA}). The figure includes the regression slope, the coefficient of determination (R^2), the statistical bias (BIAS), the root-mean-square error (RMSE), the number of observations (n), and the one-to-one line (grey dashed line).

4. Categories of atmospheric stability

Figure S1 shows the frequency distribution of the hourly calculated categories of atmospheric stability.

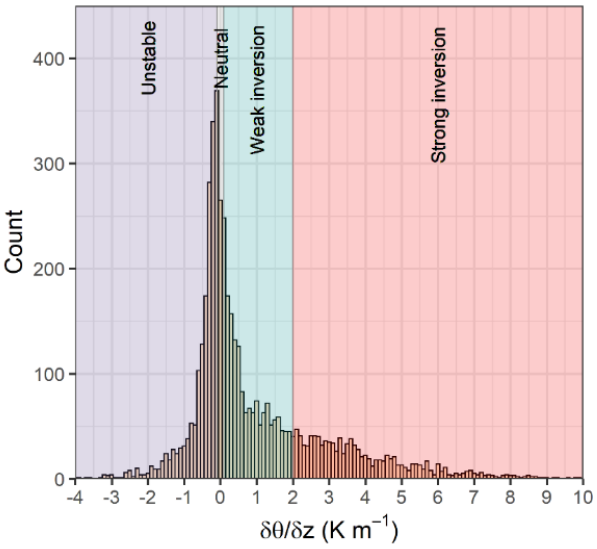

Figure S3. Frequency distribution of the potential temperature gradient ($\partial\theta/\partial z$).

5. Mie modeling

Equations for particle volumetric fractions and shell refractive index via mixing rule.

Particle mass

$$M_{Total\ particle} = M_{OC} + M_{InA} + M_{BC}, \quad \text{(S6)}$$

Particle volume fractions

$$V_{f,OC} = \frac{\frac{M_{OC}}{\rho_{OA}}}{\frac{M_{Total\ particle}}{\rho_{Total\ particle}}}, \quad \text{(S7)}$$

$$V_{f,InA} = \frac{\frac{M_{InA}}{\rho_{InA}}}{\frac{M_{Total\ particle}}{\rho_{Total\ particle}}}, \quad \text{(S8)}$$

$$V_{f,BC} = \frac{\frac{M_{BC}}{\rho_{BC}}}{\frac{M_{Total\ particle}}{\rho_{Total\ particle}}}, \quad \text{(S9)}$$

Shell refractive index:

$$k_{Shell} = \frac{(k_{OA} * V_{f,OC}) + (k_{InA} * V_{f,InA})}{(V_{f,OC} + V_{f,InA})}, \quad \text{(S10)}$$

Table S1. Complex refractive indexes of black carbon, organic aerosols and inorganic aerosols used in the Mie modeling

λ (nm)	BC		Ref	OA		Ref	InA		Ref
	n	k		n	k		n	k	
370	1.92	0.67	Kim et al., 2015	1.59	0.11	(Kim et al., 2015)	1.4	<0.01	(Shamjad et al., 2012)
470	1.92	0.67		1.47	0.11				
520	1.96	0.65		1.47	0.04				
590	1.96	0.65		1.47	0.04				
660	2	0.63		1.47	0				
880	2	0.63		1.47	0				

References

Cuesta-Mosquera, A., Mocnik, G., Drinovec, L., Müller, T., Pfeifer, S., Minguillon, M. C., Briel, B., Buckley, P., Dudoitis, V., Fernández-García, J., Fernandez-Amado, M., De Brito, J. F., Riffault, V., Flentje, H., Heffernan, E., Kalivitis, N., Kalogridis, A. C., Keernik, H., Marmureanu, L., Luoma, K., Marinoni, A., Pikridas, M., Schauer, G., Serfozo, N., Servomaa, H., Titos, G., Yus-Diez, J., Zioła, N. and Wiedensohler, A.: Intercomparison and characterization of 23 Aethalometers under laboratory and ambient air conditions: Procedures and unit-to-unit variabilities, Atmos. Meas. Tech., 14(4), 3195–3216, doi:10.5194/amt-14-3195-2021, 2021.

Digitel Enviro Sense: DIGITEL DHA-80. [online] Available from: http://www.digitel-ag.com/de/wp-content/uploads/Brochure-DHA-80-2015-EN-def.pdf, 2021.

Drinovec, L., Močnik, G., Zotter, P., Prévôt, A. S. H., Ruckstuhl, C., Coz, E., Rupakheti, M., Sciare, J., Müller, T., Wiedensohler, A. and Hansen, A. D. A.: The "dual-spot" Aethalometer: An improved measurement of aerosol black carbon with real-time loading compensation, Atmos. Meas. Tech., 8(5), 1965–1979, doi:10.5194/amt-8-1965-2015, 2015.

Drinovec, L., Jagodič, U., Pirker, L., Škarabot, M., Kurtjak, M., Vidović, K., Ferrero, L., Visser, B., Röhrbein, J., Weingartner, E., Kalbermatter, D. M., Vasilatou, K., Bühlmann, T., Pascale, C., Müller, T., Wiedensohler, A. and Močnik, G.: A dual-wavelength photothermal aerosol absorption monitor: design, calibration and performance, Atmos. Meas. Tech., 15(12), 3805–3825, doi:10.5194/amt-15-3805-2022, 2022.

Kim, J., Bauer, H., Dobovičnik, T., Hitzenberger, R., Lottin, D., Ferry, D. and Petzold, A.: Assessing optical properties and refractive index of combustion aerosol particles through combined experimental and modeling studies, Aerosol Sci. Technol., 49(5), 340–350, doi:10.1080/02786826.2015.1020996, 2015.

Magee Scientific: Aethalometer® Model AE33 User Manual, , (ver. 1.57), 149 [online] Available from: www.aerosol.eu, 2018.

Rigler, M., Drinovec, L., Lavri, G., Vlachou, A., Prevot, A. S. H., Luc Jaffrezo, J., Stavroulas, I., Sciare, J., Burger, J., Kranjc, I., Turšič, J., D. A. Hansen, A. and Mocnik, G.: The new instrument using a TC-BC (total carbon-black carbon) method for the online measurement of carbonaceous aerosols, Atmos. Meas. Tech., 13(8), 4333–4351, doi:10.5194/amt-13-4333-2020, 2020.

Shamjad, P. M., Tripathi, S. N., Aggarwal, S. G., Mishra, S. K., Joshi, M., Khan, A., Sapra, B. K. and Ram, K.: Comparison of experimental and modeled absorption enhancement by Black Carbon (BC) cored polydisperse aerosols under hygroscopic conditions, Environ. Sci. Technol., 46(15), 8082–8089, doi:10.1021/es300295v, 2012.

TSI Inc: Versatile Water-Based Condensation Particle Counter 3789, [online] Available from: https://tsi.com/products/particle-counters-and-detectors/condensation-particle-counters/versatile-water-based-condensation-particle-counter-3789/, 2023.

Wiedensohler, A.: An approximation of the bipolar charge distribution for particles i the submicron size range, J. Aerosol Sci., 19(3), 387–389, doi:10.1016/0021-8502(88)90278-9, 1988.

Wiedensohler, A., Birmili, W., Nowak, A., Sonntag, A., Weinhold, K., Merkel, M., Wehner, B., Tuch, T., Pfeifer, S., Fiebig, M., Fjäraa, A. M., Asmi, E., Sellegri, K., Depuy, R., Venzac, H., Villani, P., Laj, P., Aalto, P., Ogren, J. A., Swietlicki, E., Williams, P., Roldin, P., Quincey, P., Hüglin, C., Fierz-Schmidhauser, R., Gysel, M., Weingartner, E., Riccobono, F., Santos, S., Grüning, C., Faloon, K., Beddows, D., Harrison, R., Monahan, C., Jennings, S. G., O'Dowd, C. D., Marinoni, A., Horn, H. G., Keck, L., Jiang, J., Scheckman, J., McMurry, P. H., Deng, Z., Zhao, C. S., Moerman, M., Henzing, B., De Leeuw, G., Löschau, G. and Bastian, S.: Mobility particle size spectrometers: Harmonization of technical standards and data structure to facilitate high quality long-term observations of atmospheric particle number size distributions, Atmos. Meas. Tech., 5(3), 657–685, doi:10.5194/amt-5-657-2012, 2012.

Wiedensohler, A., Wiesner, A., Weinhold, K., Birmili, W., Hermann, M., Merkel, M., Müller, T., Pfeifer, S., Schmidt, A., Tuch, T., Velarde, F., Quincey, P., Seeger, S. and Nowak, A.: Mobility particle size spectrometers: Calibration procedures and measurement uncertainties, Aerosol Sci. Technol., 52(2), 146–164, doi:10.1080/02786826.2017.1387229, 2018.